$N = 8$ Shell Breaking in ^{12}Be from a Single-Particle Perspective

J. Chen,[1,2,*] B. P. Kay,[2] D. K. Sharp,[3] L. P. Gaffney,[4] S. J. Freeman,[3,5] S. M. Wang,[6,7] J. G. Li,[8,9,10] P. T. MacGregor,[3,5] C. R. Hoffman,[2] Y. Ayyad,[11] P. A. Butler,[4] S. Carollo,[12,13] A. Ceulemans,[14] D. J. Clarke,[3] A. J. Dolan,[4] C. Everett,[4] Z. Favier,[5] K. Garrett,[3] J. Geng,[15] H. Jayatissa,[2] M. Labiche,[16] I. Lazarus,[16] W. P. Liu,[1] Y. F. Niu,[15] B. Olaizola,[5,17] J. Ojala,[4] C. A. A. Page,[18,5] R. D. Page,[4] O. Poleshchuk,[14] R. Raabe,[14] M. R. Xie,[8,9] C. X. Yuan,[19] Z. Yue,[18,5] and Y. N. Zhang[19]

(ISOLDE Collaboration)

[1]*Department of Physics, Southern University of Science and Technology, Shenzhen, 518055, Guangdong, China*
[2]*Physics Division, Argonne National Laboratory, Lemont, Illinois 60439, USA*
[3]*Department of Physics, University of Manchester, M13 9PL Manchester, United Kingdom*
[4]*Department of Physics, University of Liverpool, Liverpool L69 3BX, United Kingdom*
[5]*EP Department, CERN, Geneva CH-1211, Switzerland*
[6]*Key Laboratory of Nuclear Physics and Ion-beam Application (MOE), Institute of Modern Physics, Fudan University, Shanghai 200433, China*
[7]*Shanghai Research Center for Theoretical Nuclear Physics, NSFC and Fudan University, Shanghai 200438, China*
[8]*Heavy Ion Science and Technology Key Laboratory, Institute of Modern Physics, Chinese Academy of Sciences, Lanzhou 730000, China*
[9]*School of Nuclear Science and Technology, University of Chinese Academy of Sciences, Beijing 100049, China*
[10]*Southern Center for Nuclear-Science Theory (SCNT), Institute of Modern Physics, Chinese Academy of Sciences, Huizhou 516000, China*
[11]*IGFAE, Universidade de Santiago de Compostela, E-15782, Santiago de Compostela, Spain*
[12]*Dipartimento di Fisica e Astronomia, Universit degli Studi di Padova, I-35131 Padova, Italy*
[13]*Istituto Nazionale di Fisica Nucleare (INFN), Sezione di Padova, Padova, Italy*
[14]*KU Leuven, Intituut voor Kern-en Stralingsfysica, Celestijnenlaan 200D, 3001 Leuven, Belgium*
[15]*Frontier Science Center for Rare Isotopes, Lanzhou University, Lanzhou 730000, China*
[16]*Nuclear Physics Group, STFC Daresbury Laboratory, Daresbury, Warrington WA4 4AD, United Kingdom*
[17]*Instituto de Estructura de la Materia, CSIC, E-28006 Madrid, Spain*
[18]*School of Physics, University of York, York YO10 5DD, North Yorkshire, United Kingdom*
[19]*Sino-French Institute of Nuclear Engineering and Technology, Sun Yat-Sen University, Zhuhai 519082, China*

(Received 9 September 2025; accepted 21 April 2026; published 2 June 2026)

Experimental observations of the low-lying states in ^{12}Be and their accurate modeling play an essential role in understanding the disappearance of the $N = 8$ magic number. Long-standing experimental ambiguities have been clarified using an one-neutron adding (d, p) reaction on ^{11}Be using the ISOLDE Solenoidal Spectrometer at CERN's HIE-ISOLDE facility. The single-particle energies of $1s_{1/2}$, $0d_{5/2}$, and $0p_{1/2}$ orbitals in ^{12}Be have been determined from the extracted spectroscopic factors. A significant reduction between the separation of $1s_{1/2}$ and $0p_{1/2}$ orbitals is found in comparison with the carbon isotones, highlighting the breakdown of the $N = 8$ shell. These observations serve as an important test of different effects incorporated in theoretical models. It is found that two synergistic mechanisms, core deformation and weak binding, are responsible for the $N = 8$ shell breaking and the exotic near-threshold phenomena observed in ^{12}Be, including the narrow unnatural-parity resonance 0^-_1 and the possible halolike nature of the 0^+_2 isomer.

DOI: 10.1103/3vts-dwst

*Contact author: chenjie@sustech.edu.cn

Introduction—The shell model introduced by Mayer and Jensen [1,2] over 75 years ago has been enormously successful in describing the nuclear structure of stable nuclei. It assumes nucleons move within an average potential and arrange themselves in single-particle orbitals akin to electrons in atoms. These orbitals are grouped into shell structures characterized by magic numbers [3].

However, in nuclei far from stability, a migration of magic numbers has been revealed through the rearrangement of single-particle orbitals [4,5]. Such shell evolution is observed to be particularly dramatic in weakly bound light nuclei, which behave as open quantum systems. This dissolving of boundary leads to a series of novel phenomena, including neutron halos [4], new magicity [5], and clusters [6].

One textbook example is the one-neutron halo nucleus ^{11}Be [7–10], whose ground state spin and parity $(1/2^+)$ contradicts conventional shell-model predictions (expected to be $1/2^-$). This system exhibits one of the lowest neutron separation energies ($S_n = 0.504$ MeV) among weakly bound nuclei, and has a dominant overlap with the ^{10}Be ground state indicated by the large neutron $1s_{1/2}$ spectroscopic factor [8]. Neighboring ^{12}Be, though more bound ($S_n = 3.16$ MeV), also demonstrates the lightest island of inversion through its low-lying excited states and enhanced B(E2) value [11–16].

Intensive theoretical efforts have been made to understand the origin of shell evolution. Specifically, it is apparent that three-body forces establish new neutron magic numbers 14 and 16 in oxygen [17], whereas deformation impacts the $N = 20$ magic number in $Z = 10$–12 nuclei [18]. In heavier systems, the tensor force plays a crucial role [19]. In addition, weak-binding effects can significantly impact the ordering of single-particle orbitals [20–22], motivating a great deal of theoretical activity [23–25] over the last few decades. Nevertheless, the mechanism for the vanishing of the $N = 8$ magic number in ^{11}Be and ^{12}Be remains contentious and lacks a unified and coherent interpretation, though various competing mechanisms have been proposed, including vibration coupling, core excitation, cluster structures, and pairing [26–30].

^{11}Be and ^{12}Be provide excellent cases for studying the open quantum phenomena under the interplay of various effects since they exhibit a multitude of exotic structure phenomena, including weak-binding effects and thus having dilute matter distributions (halos), deformation due to molecularlike cluster structures [31], and the cross-shell configuration mixing. Furthermore, the small number of nucleons involved facilitates an in-depth theoretical study of these effects with relatively simple assumptions. However, despite numerous experimental efforts [11–15,32–39], the structure of low-lying states in ^{12}Be remains poorly understood. For example, it is not clear how the $1s_{1/2}$, $0p_{1/2}$, and $0d_{5/2}$ orbitals evolve in the region nearby and how the above-mentioned phenomena affect them. In particular, there is little consensus on the nature of the unbound states [15,28,29,36,38–44]. A more complete description of ^{12}Be remains highly desirable to advance understanding of how open quantum systems behave under various effects.

One-neutron transfer reactions serve as an insightful experimental probe for shell evolution, where the differential cross sections with respect to angles reveal the underlying single-particle structure and thus can directly challenge the various assumptions incorporated in the theoretical models. Over the past two decades, there have been three measurements of the ^{11}Be$(d, p)^{12}$Be reaction [35–37], but each with its own limitations in terms of resolution, statistics, or beam energy (too high or too low for $1n$-transfer reactions), leaving considerable uncertainties.

In this Letter, we report on a new measurement of the ^{11}Be$(d, p)^{12}$Be reaction at a beam energy of 9.78 MeV/u. At this energy, the cross sections can be reliably understood with theoretical models that assume a direct, single-step mechanism for the transfer of a neutron. The superior Q-value resolution obtained in this measurement has enabled the first direct determination of the s-wave spectroscopic factors of the isomeric 0_2^+ state, supporting the hypothesis that this state has a two-neutron halo structure. In addition, the excitation energies (to less than 10 keV uncertainty) and widths of the 0_1^- and 2_1^- resonances have been determined for the first time. The single-particle energies of the $1s_{1/2}$, $0p_{1/2}$, and $0d_{5/2}$ orbitals were inferred and show a similar trend to those in ^{11}Be while a sharp distinction to the C isotones. The specific synergy between collectivity and continuum coupling is essential for successfully describing the properties of ^{12}Be and plays a significant role in the breaking of the $N = 8$ shell closure. It stands out as an example showing that the interplay of internal structure and external coupling results in dramatic reordering of quantum states (see Refs. [45,46] for examples).

Experiment—The experiment was carried out at the HIE-ISOLDE Linac beam facility at CERN utilizing the ISOLDE Solenoidal Spectrometer (ISS). A beam of ^{11}Be at 9.78 MeV/u was delivered with an intensity of $\sim 10^6$ particles per second onto a deuterated-polyethylene (CD_2) target of 120(8) $\mu g/cm^2$ thickness (with a hydrogen content less than 10%). There was 3% ^{22}Ne contamination in the beam, which was separated from the ^{11}Be in the analysis (see below). Outgoing protons were transported by the 2.0-T magnetic field of ISS, returning to the beam axis and detected by the newly constructed ISS silicon detector array. The ISS silicon array has a hexagonal cross section and an overall length of 0.5 m. Each face of the array features four double-sided silicon-strip detectors (DSSSDs), each with 128 strips of 0.95-mm pitch on the front and 11 strips of 2-mm pitch on the back. The positions at which the protons return to the beam axis were determined with these DSSSDs. This silicon array was positioned upstream of the target, 90 mm from the target to the edge of the nearest detector, corresponding to a c.m. angular range of $12° \lesssim \theta_{cm} \lesssim 40°$ for protons populating low-lying states in ^{12}Be. An annular silicon detector positioned 153 mm downstream of the target (corresponding to $\theta_{cm} \sim 20°$) was used to monitor ions elastically scattered from the target [47]. The absolute cross sections were determined with about 15% uncertainty, normalized

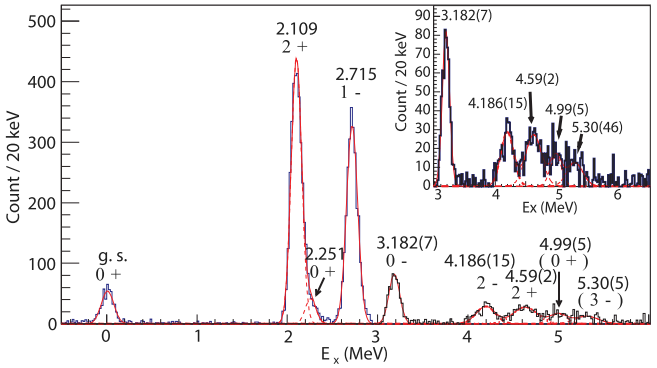

FIG. 1. Excitation spectrum of ^{12}Be populated via the ^{11}Be$(d, p)^{12}$Be reaction. The spectrum represents protons collected over $-520 < z < -90$ mm and gated on the Be recoils, which corresponds to $\theta_{cm} \sim 12° - 40°$. The peaks are labeled by their excitation energies (in MeV) together with their spin-parity assignments. The inset shows the details of the resonances with a dominant one-neutron decay branch.

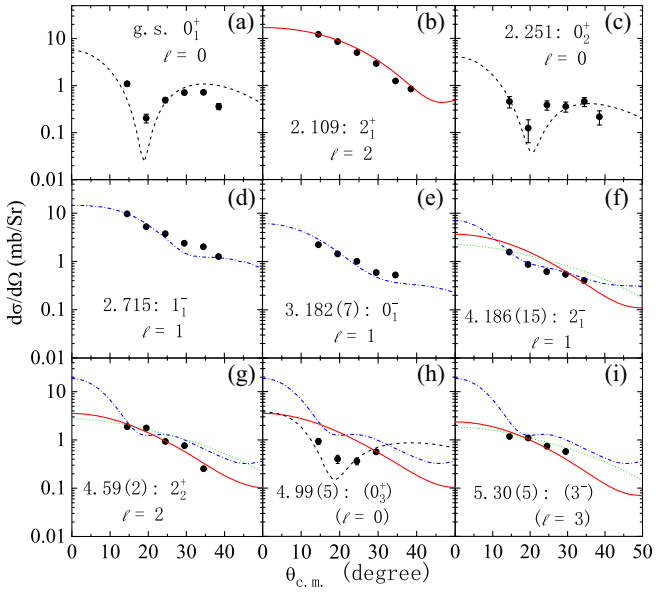

FIG. 2. Differential cross sections of the ^{11}Be$(d, p)^{12}$Be reaction. Results of the DWBA calculations are compared to the data with the excitation energies (in MeV), spin parities, and adopted ℓ values labeled. For some states without spin-parity assignment before, $\ell = 0$ (black dashed lines), $\ell = 1$ (blue dotted-dashed lines), $\ell = 2$ (red solid lines), and $\ell = 3$ (green dotted lines) angular distributions are shown.

by the elastically scattered deuterons. A set of recoil detectors, consisting of 65-μm (energy loss, ΔE) and 500-μm (residual energy, E) thick quadrant silicon detectors, was placed 610 mm downstream of the target. These recoil detectors have an inner and outer radius of 9 mm and 45 mm, respectively, with $> 70\%$ acceptance for the recoils of interest. This acceptance was determined and corrected by a realistic simulation including the neutron decay process. Using the particle identification in the recoil detectors, the beam contamination and the decay branching ratios for the unbound states were determined. Background from random coincidences with protons was further eliminated using timing coincidences between recoils and the silicon array.

Figure 1 shows the excitation energy spectrum of ^{12}Be, as populated in the ^{11}Be(d, p) reaction, identified by the timing coincidence between the recoil detectors and the silicon array. A Q-value resolution of ~140 keV (full width at half maximum) was achieved. Bound and unbound states decaying through one- and two-neutron emissions were identified with the coincidence of ^{12}Be, ^{11}Be, and ^{10}Be, respectively. The differential cross sections have been determined for excited states up to $E_x = 5.4$ MeV at approximately ~5° increments over the angular range covered. The θ_{cm} angles were derived from the position of the protons along the beam axis. The Q-value resolution is just sufficient to separate the 2_1^+ (2.109 MeV) and 0_2^+ (2.251 MeV) states [48], and their angular distributions were resolved by fitting the doublet at each angular bin. The uncertainties for the 2_1^+ and 0_2^+ states include both fitting and statistical errors, while the uncertainties for other states are purely statistical.

In Fig. 2, the experimental angular distributions are compared to distorted-wave Born approximation (DWBA) calculations performed using PTOLEMY [49] with global optical parameters in Refs. [50,51]. They were derived from systems close in mass and have been successfully applied to light nuclei near this region [52,53]. Transitions to the unbound states were calculated with DWUCK5 [54] following the prescription of Ref. [55]. Four known bound states in ^{12}Be have been populated, including the ground state, 2.11-, 2.25-, and 2.72-MeV states, associated with the angular momentum of $\ell = 0$, 2, 0, and 1, respectively.

A resonance at 3.182(7) MeV is just 12 keV above the one-neutron separation energy ($S_n = 3.170$ MeV). The signature of this near-threshold resonance was observed in Ref. [56]. However, the energy resolution of the previous measurement did not allow for the explicit determination of its excitation energy and width. In the present measurement, it is determined to be at 3.182(7) MeV in excitation energy, with a width of < 30 keV. The neutron decay branching ratio is determined to be at least 98% based on the ratio of ^{11}Be and ^{12}Be observed in the recoil detectors. Over the past decades, prior to its observation, there has been much theoretical speculation devoted to this near-threshold $1p$-$1h$ 0^- resonance [28,29,41–43]: it has now been firmly determined as a new example of threshold "aligned" states (see details in Refs. [56,57]).

Three additional resonances were observed above the two-neutron emission threshold ($S_{2n} = 3.672$ MeV), located at 4.186(15), 4.59(2), and 4.99(5) MeV. It was noted that all these resonances predominantly exhibit one-neutron decay. The 4.186(15) MeV state was observed as an $\ell = 1$ angular momentum transition for the first time,

TABLE I. Excitation energies E_x, transferred orbital angular momentum ℓ, spin-parities J^π, shell-model orbital $n\ell s$, spectroscopic factors S, and widths Γ for the low-lying states in ^{12}Be observed in the present ^{11}Be$(d,p)^{12}$Be reaction.

E_x(MeV)	ℓ	J^π	$n\ell s$	S	Γ(MeV)
ground state	0	0^+	$1s_{1/2}$	0.3(3)	⋯
2.109	2	2^+	$0d_{5/2}$	0.45(4)	⋯
2.251	0	0_2^+	$1s_{1/2}$	0.39(6)	⋯
2.715	1	1^-	$0p_{1/2}$	0.72(6)	⋯
3.182(7)	1	0^-	$0p_{1/2}$	0.71(7)	<0.03
4.186(15)	1	2^-	$0p_{3/2}$	0.09(1)	0.13(4)
4.59(2)	2	2_2^+	$0d_{5/2,3/2}$	0.04(1)	0.17(7)
4.99(5)	(0)	(0_3^+)	$(1s_{1/2})$	0.7(2)	0.15(7)
5.30(5)	(2, 3)	$(2^+, 3^-)$	$(0d_{5/2,3/2}, 0f_{7/2})$		

with 2_1^- being the tentative assignment. For the 4.59 (2) MeV state, there has been extensive discussion about its spin parity [38,43], focusing primarily on 2_2^+ or 3_1^-. Its angular distribution in this Letter is consistent with $\ell = 2$, leading to the assignment of 2_2^+. A recent ^{10}Be$(t,p)^{12}$Be measurement [58] indicated 3_1^-, suggesting the presence of a doublet at ≈4.6 MeV. The 4.99(5) MeV resonance is tentatively assigned as the third 0^+ state, corroborated by the recent ^{10}Be$(t,p)^{12}$Be measurement [58] and supported by theory as discussed below.

The spectroscopic factors of these states were obtained by normalization of the experimental differential cross sections to the calculated ones and are shown in Table I and in Fig. 3(a). The uncertainties of the absolute and relative spectroscopic factors are estimated to be about 18%–25% and 5%–10%, respectively, taking into account the variation in the global optical model parameters and the normalization uncertainty. The sum of the spectroscopic factors for the ground state and isomeric 0_2^+ state is 0.69(9), which is well below the expected sum of the $1s_{1/2}$ spectroscopic factors ($\sum S_{1s1/2} = 2.0$), indicating missing $1s_{1/2}$ strength. Given the breakdown of the $N = 8$ shell closure, a third 0^+ state is expected due to the configuration mixing of two neutrons in the $1s_{1/2}$, $0p_{1/2}$, and $0d_{5/2}$ orbitals [36,59]. The observed resonance at 4.99(5) MeV is likely the third 0^+ state based on the angular distribution, the result of Ref. [58], and these theoretical expectations. The spectroscopic factor was estimated to be 0.7(2) and results in a quenching factor of 0.7(2) [60] for the $1s_{1/2}$ strength. The centroid of the $1s_{1/2}$ strength was determined to be 3.15 MeV using the equation $E_{\text{centroid}} = (\sum (2J+1) S_{\ell J} \times E_{ex} / \sum (2J+1) S_{\ell J})$ [61]. For the $0p_{1/2}$ orbital, the centroid was determined to be 2.85 MeV, based on the spectroscopic factors of the 1_1^- and 0_1^- states. The summed strength nearly exhausts the $0p_{1/2}$ strength, with a quenching factor of 0.7(1). The centroid of the $0d_{5/2}$ orbital should be determined by a set of 2^+ and 3^+ states.

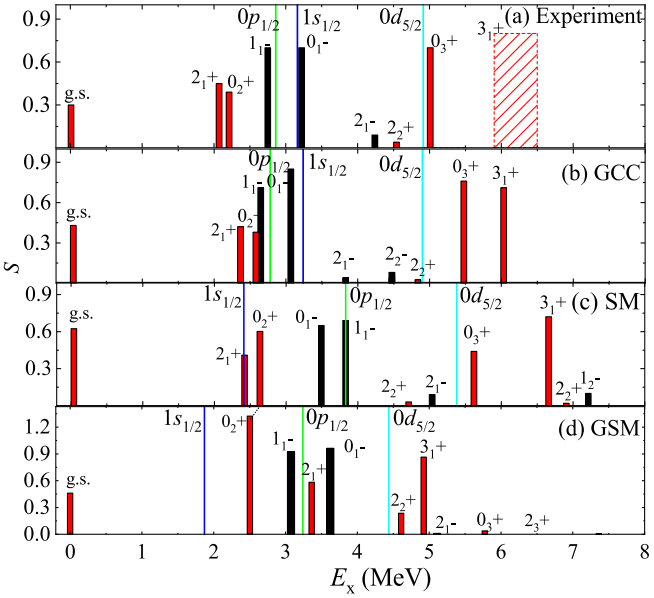

FIG. 3. Experimental spectroscopic factors of low-lying states in ^{12}Be populated via the ^{11}Be$(d,p)^{12}$Be reaction (a), in comparison with the calculated results of the shell model (SM) with the YSOX interaction (c), the GSM (d), and the GCC (b) approach. The red and black bars represent the spectroscopic factors of the positive and negative-parity states, respectively. The single-particle energies of the $1s_{1/2}$ (dark blue), $0p_{1/2}$ (green), and $0d_{5/2}$ (light blue) are plotted as vertical lines in each case. The hatched bar indicates experimental limits on the location and strength of the 3^+ state inferred in this Letter.

While the first two 2^+ states were observed, the 3^+ state is likely to exist around 6 MeV according to most theoretical models and previous experiments [36,62], which is outside the range explored in this measurement. The lower limit of the $0d_{5/2}$ strength in the 3^+ state was estimated using an average quenching factor of 0.7, based on the strengths of the $1s_{1/2}$ and $0p_{1/2}$ orbitals. Thus, the single-particle energy of the $0d_{5/2}$ orbital is estimated to be around 4.7–5.3 MeV. Conservatively speaking, these single-particle energies determined from the centroids have uncertainties of about ±200–300 keV [20,22]. It is worth noting that the discussion below is not impacted by the relatively larger uncertainties of the absolute spectroscopic factors.

Discussion—The spectroscopic factors have been compared with the results of shell-model calculations using the YSOX interaction [63] [Fig. 3(c)], which is optimized for *psd*-shell nuclei and can reproduce the shell inversion in ^{11}Be. However, the excitation energies of the excited states are overestimated, particularly for the negative-parity states. Moreover, in this calculation, the single-particle energies of the $0p_{1/2}$ orbital derived from the centroids are about 1.42 MeV higher than those of the $1s_{1/2}$ orbital, yet significantly lower than those of the $0d_{5/2}$ orbital (around 5.3 MeV). Attempts to adjust the energy of the $0p_{1/2}$ orbital

to match experimental single-particle energies fail to reproduce the inversion order of the $1/2^+$ and $1/2^-$ states in ^{11}Be. In addition, it substantially underestimates the binding energy of ^{10}Be. These discrepancies likely originate from the limited model space, which can not capture deformation and weak-binding effects.

To incorporate the continuum coupling effect, calculations with the Gamow shell model (GSM) [24] and Gamow coupled channel approach (GCC) [25] were performed. The resulting spectroscopic factors and single-particle energies are shown in Figs. 3(b) and 3(d), respectively. The GSM calculation, which assumes ^{8}He as a closed core and uses a fitted interaction, overestimates the spectroscopic factor of the second 0^+ state by a factor of 4, resulting in a much lower $1s_{1/2}$ orbital compared to the $0p_{1/2}$ orbital. However, adjusting the $1s_{1/2}$ orbital upward inverted the level order of ^{11}Be, similarly to the shell model. This discrepancy suggests the necessity of core excitation beyond a rigid ^{8}He core.

The GCC approach offers an alternative approach by integrating the deformation of the ^{10}Be core and continuum coupling effects [64]. This model yields the best agreement with experimental data, both in terms of excitation energies and spectroscopic factors. The GCC calculation shows that the single-particle energy of the $1s_{1/2}$ orbital is considerably higher than those from the other two models, nearly degenerate with the $0p_{1/2}$ orbital, which aligns more closely with experimental data. This improvement likely stems from the fact that the GCC model accounts for continuum coupling effects *and* the proper treatment of the deformed ^{10}Be core [65]. Attempts to reduce core deformation by adjusting the 2^+ energy fail to reproduce the experimental result. Consequently, the low-lying states of ^{12}Be reflect a deformed ^{10}Be core coupled with two valence neutrons with weak-binding effects, which are well represented in the calculations.

The deduced single-particle energies of the $1s_{1/2}$ and the $0p_{1/2}$ orbitals appear nearly degenerate and lie in close proximity to S_n, while the $0d_{5/2}$ orbital resides approximately 2 MeV higher (see Fig. 4). This energy hierarchy mirrors the pattern observed in ^{11}Be, suggesting evolutionary continuity in single-particle structures across these systems. The enlarged energy gap between $1s_{1/2}$ and the $0d_{5/2}$ orbital compared to the carbon isotopes is an indication of the weak-binding effect—the rate at which the $1s_{1/2}$ orbital approaches the particle emission threshold is considerably slower than that of the $0d_{5/2}$ orbital (which has a $\ell = 2$ barrier to overcome), and thus its energy becomes significantly lowered relative to the $0d_{5/2}$ orbital in ^{11,12}Be.

A striking reduction in the energy separation (Δ_{sp}) between the $0p_{1/2}$ and $1s_{1/2}$ orbitals compared with carbon isotones (Fig. 4) drives the intrusion of the $N = 8$ shell

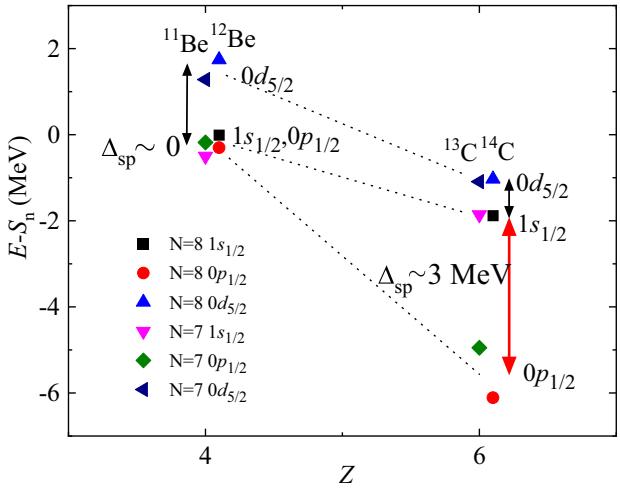

FIG. 4. Experimental binding energies of the neutron $1s_{1/2}$, $0d_{5/2}$, $0p_{1/2}$ orbitals of $N = 7$, 8 Be and C isotopes (deduced with present Letter and information from [48]). The single-particle separation of $1s_{1/2}$-$0d_{5/2}$ and $1s_{1/2}$-$0p_{1/2}$ (with Δ_{sp} values labeled) are labeled by black and red arrows, respectively.

closure. Analysis using a deformed Woods-Saxon potential reveals that the energy separation between $1/2_2^+$ and $1/2_1^-$ Nilsson orbits reduces by over 3 MeV between C and Be, driven in part by large deformation changes. In this model, the $1/2_2^+$ state evolves to carry a dominant fraction of the $1s_{1/2}$ strength as its binding energy approaches zero and becomes almost degenerate with $0p_{1/2}$, which reproduces the observation in the present experiment. This interplay between deformation and threshold proximity drives the large Δ_{sp} reduction revealed in the present Letter, and is of fundamental significance to the breakdown of $N = 8$ shell closure as well as the formation of neutron halo in ^{11}Be [66].

This shell breaking drives exotic phenomena near the neutron-emission threshold of ^{12}Be via continuum coupling. Particularly noteworthy is the emergence of a narrow 0^- resonance just above threshold, corresponding to a cross-shell $1p$-$1h$ excitation enhanced by the threshold "alignment" effect [57]. Furthermore, our calculations using the method from Ref. [67] reveal that the isomeric 0_2^+ state possesses an enlarged matter radius of 2.76 fm compared to 2.59(6) fm of the ground state [68], suggesting halo formation in the 0_2^+ state of ^{12}Be. It stems from a reduction in the d-wave component ($57\%p^2$ and $16\%s^2$ is dominant) combined with its proximity to the threshold. This also agrees with the observation of Ref. [69] that an appreciable weak-binding s or p component can result in an obvious enhancement in the matter radius. A direct measurement of 0_2^+ radius using an isomer beam is still eagerly awaited.

In summary, the one-neutron adding reaction on ^{11}Be has been carried out to clarify the long-standing ambiguities in ^{12}Be. The single-particle energies of the $0p_{1/2}$, $0d_{5/2}$, and $1s_{1/2}$ have been inferred and show dramatic evolution to

the C isotones. By comparing the experimental result to the theoretical calculation, it was found that accurate modeling of ^{12}Be requires both continuum-coupling effects and deformation, which drive the intrusion of the *sd* orbitals into the *p* shell and the breakdown of $N = 8$. These effects bring in rich exotic phenomena in the description of the low-lying states of ^{12}Be, including the possible two-neutron halo structure in the isomeric 0_2^+ state and the cross-shell $1p$-$1h$ narrow 0^- resonance near the threshold.

Acknowledgments—The authors would like to acknowledge the operation staff at ISOLDE for providing the beam. This material is based upon work supported by the U.S. Department of Energy, Office of Science, Office of Nuclear Physics, under Contract No. DEAC02-06CH11357 (Argonne); National Natural Science Foundation of China under Contracts No. 12475120, No. 12147101, No. 12475129, and No. 12435010; the U.K. Science and Technology Facilities Council (Grants No. ST/P004423/1, No. ST/R004056/1, No. ST/V001027/1, No. ST/V001116/1, No. ST/y000323/1, No. ST/T004797/1 and No. ST/Y000242/1. Y. A. is supported by Grants No. RYC2019-028438-I and No. PID2021-125995NA-I00 funded by MCIN/AEI/10.13039/501100011033 and by the Regional Government of Galicia under the program "Proyectos de excelencia" Grant No. ED431F 2022/13.

Data availability—The data that support the findings of this article are openly available [70], embargo periods may apply.

[1] M. G. Mayer, Phys. Rev. **75**, 1969 (1949).
[2] O. Haxel, J. H. D. Jensen, and H. E. Suess, Phys. Rev. **75**, 1766 (1949).
[3] M. Mayer and J. Jensen, Elementary Theory of Nuclear Shell Structure, Structure of Matter Series (John Wiley & Sons, New York, 1955); M. G. Mayer, Phys. Rev. **78**, 22 (1950).
[4] I. Tanihata, H. Savajols, and R. Kanungo, Prog. Part. Nucl. Phys. **68**, 215 (2013); I. Tanihata, H. Hamagaki, O. Hashimoto *et al.*, Phys. Lett. **160B**, 380 (1985).
[5] B. A. Brown, Physics **4**, 525 (2022).
[6] M. Freer, H. Horiuchi, Y. Kanada-En'yo, D. Lee, and U. G. Meissner, Rev. Mod. Phys. **90**, 035004 (2018).
[7] I. Talmi and I. Unna, Phys. Rev. Lett. **4**, 469 (1960).
[8] K. T. Schmitt *et al.*, Phys. Rev. Lett. **108**, 192701 (2012).
[9] T. Aumann *et al.*, Phys. Rev. Lett. **84**, 35 (2000).
[10] I. Tanihata, T. Kobayashi, O. Yamakawa, S. Shimoura, K. Ekuni, K. Sugimoto, N. Takahashi, T. Shimoda, and H. Sato, Phys. Lett. B **206**, 592 (1988).
[11] H. Iwasaki, T. Motobayashi, H. Akiyoshi *et al.*, Phys. Lett. B **491**, 8 (2000).
[12] H. Iwasaki *et al.*, Phys. Lett. B **481**, 7 (2000).
[13] S. Shimoura, A. Saito, T. Minemura *et al.*, Phys. Lett. B **560**, 31 (2003).
[14] N. Imai *et al.*, Phys. Lett. B **673**, 179 (2009).
[15] D. E. Alburger, D. P. Balamuth, J. M. Lind, L. Mulligan, K. C. Young, Jr., R. W. Zurmühle, and R. Middleton, Phys. Rev. C **17**, 1525 (1978).
[16] H. T. Fortune, G.-B. Liu, and D. E. Alburger, Phys. Rev. C **50**, 1355 (1994).
[17] T. Otsuka, T. Suzuki, J. D. Holt, A. Schwenk, and Y. Akaishi, Phys. Rev. Lett. **105**, 032501 (2010).
[18] N. Tsunoda, T. Otsuka, K. Takayanagi, N. Shimizu, T. Suzuki, Y. Utsuno, S. Yoshida, and H. Ueno, Nature (London) **587**, 66 (2020).
[19] T. Otsuka, T. Suzuki, R. Fujimoto, H. Grawe, and Y. Akaishi, Phys. Rev. Lett. **95**, 232502 (2005).
[20] B. P. Kay, C. R. Hoffman, and A. O. Macchiavelli, Phys. Rev. Lett. **119**, 182502 (2017).
[21] C. R. Hoffman, B. P. Kay, and J. P. Schiffer, Phys. Rev. C **89**, 061305(R) (2014).
[22] J. Chen, B. P. Kay, C. R. Hoffman *et al.*, Phys. Lett. B **853**, 138678 (2024).
[23] J. Okołowicz, M. Płoszajczak, and I. Rotter, Phys. Rep. **374**, 271 (2003).
[24] N. Michel and M. Płoszajczak, *Gamow Shell Model, The Unified Theory of Nuclear Structure and Reactions*, Lecture Notes in Physics Vol. 983 (Springer, Cham, 2021).
[25] S. M. Wang and W. Nazarewicz, Phys. Rev. Lett. **126**, 142501 (2021).
[26] G. Gori, F. Barranco, E. Vigezzi, and R. A. Broglia, Phys. Rev. C **69**, 041302(R) (2004).
[27] F. M. Nunes, I. J. Thompson, and J. A. Tostevin, Nucl. Phys. **A703**, 593 (2002).
[28] G. Blanchon, N. V. Mau, A. Bonaccorso, M. Dupuis, and N. Pillet, Phys. Rev. C **82**, 034313 (2010).
[29] Y. Kanada-En'yo and H. Horiuchi, Phys. Rev. C **68**, 014319 (2003).
[30] J. Geng, P. W. Zhao, Y. F. Niu, and W. H. Long, Phys. Lett. B **858**, 139036 (2024).
[31] Z. H. Yang, Y. L. Ye, Z. H. Li *et al.*, Phys. Rev. Lett. **112**, 162501 (2014).
[32] A. Navin, D. W. Anthony, T. Aumann *et al.*, Phys. Rev. Lett. **85**, 266 (2000).
[33] S. D. Pain, W. N. Catford, N. A. Orr *et al.*, Phys. Rev. Lett. **96**, 032502 (2006).
[34] R. Meharchand, R. G. T. Zegers, B. A. Brown *et al.*, Phys. Rev. Lett. **108**, 122501 (2012).
[35] R. Kanungo, A. T. Gallant, M. Uchida *et al.*, Phys. Lett. B **682**, 391 (2010).
[36] J. Chen, J. L. Lou, Y. L. Ye *et al.*, Phys. Lett. B **781**, 412 (2018).
[37] J. G. Johansen, V. Bildstein, M. J. G. Borge *et al.*, Phys. Rev. C **88**, 044619 (2013).
[38] W. Liu, J. L. Lou, Y. L. Ye, S. M. Wang *et al.*, Phys. Rev. C **105**, 034613 (2022).
[39] J. K. Smith, T. Baumann, D. Bazin *et al.*, Phys. Rev. C **90**, 024309 (2014).
[40] H. T. Fortune, Phys. Lett. B **755**, 351 (2016).
[41] E. Garrido, A. S. Jensen, D. V. Fedorov, and J. G. Johansen, Phys. Rev. C **86**, 024310 (2012).
[42] C. Romero-Redondo, E. Garrido, D. V. Fedorov, and A. S. Jensen, Phys. Rev. C **77**, 054313 (2008).

[43] H. T. Fortune, Phys. Rev. C **89**, 017302 (2014).
[44] C. Romero-Redondo, E. Garrido, D. V. Fedorov, and A. S. Jensen, Phys. Lett. B **660**, 32 (2008).
[45] Cheng Chin, Rudolf Grimm, Paul Julienne, and Eite Tiesinga, Rev. Mod. Phys. **82**, 1225 (2010).
[46] A. Krasnok, A. Slobozhanyuk, C. Simovski, S. A. Tretyakov, A. N. Poddubny, A. E. Miroshnichenko, Y. S. Kivshar, and P. A. Belov, Sci. Rep. **5**, 12956 (2015).
[47] C. R. Hoffman, B. B. Back, B. P. Kay *et al.*, Phys. Rev. C **85**, 054318 (2012).
[48] https://www.nndc.bnl.gov/.
[49] M. H. Macfarlane and S. C. Pieper, Argonne National Laboratory Report No. ANL-500 76-11 Rev. 1 (1978).
[50] A. J. Koning and J. P. Delaroche, Nucl. Phys. **A713**, 231 (2003).
[51] H. An and C. Cai, Phys. Rev. C **73**, 054605 (2006).
[52] J. Chen *et al.*, Phys. Rev. C **100**, 064314 (2019).
[53] B. P. Kay, T. L. Tang, I. A. Tolstukhin *et al.*, Phys. Rev. Lett. **129**, 152501 (2022).
[54] P. D. Kunz, DWUCKS: Nuclear Model Code System for Distorted Wave Born Approximation and Coupled Channel Calculations, 10.2172/4157791.
[55] C. M. Vincent and H. T. Fortune, Phys. Rev. C **2**, 782 (1970).
[56] J. Chen, S. M. Wang, H. T. Fortune, J. L. Lou *et al.*, Phys. Rev. C **103**, L031302 (2021).
[57] J. Okołowicz, M. Płoszajczak, and W. Nazarewicz, Phys. Rev. Lett. **124**, 042502 (2020).
[58] B. P. Kay *et al.* (private communication).
[59] F. C. Barker, J. Phys. G **2**, L45 (1976).
[60] B. P. Kay, J. P. Schiffer, and S. J. Freeman, Phys. Rev. Lett. **111**, 042502 (2013).
[61] M. Baranger, Nucl. Phys. **A149**, 225 (1970).
[62] H. T. Fortune, Phys. Rev. C **104**, 014314 (2021).
[63] C. Yuan, T. Suzuki, T. Otsuka, F. Xu, and N. Tsunoda, Phys. Rev. C **85**, 064324 (2012).
[64] S. M. Wang, W. Nazarewicz, R. J. Charity, and L. G. Sobotka, Phys. Rev. C **99**, 054302 (2019).
[65] J. Chen, Y. Ayyad, D. Bazin, W. Mittig *et al.*, Phys. Rev. Lett. **134**, 012502 (2025).
[66] I. Hamamoto and S. Shimoura, J. Phys. G **34**, 2715 (2007).
[67] H. T. Fortune and R. Sherr, Phys. Rev. C **86**, 064322 (2012).
[68] A. Krieger, K. Blaum, M. L. Bissell *et al.*, Phys. Rev. Lett. **108**, 142501 (2012).
[69] Z. H. Yang, Y. Kubota, A. Corsi *et al.*, Phys. Rev. Lett. **126**, 082501 (2021).
[70] 10.5281/zenodo.17015031.